ISSN 1062-8738, Bulletin of the Russian Academy of Sciences. Physics, 2015, Vol. 79, No. 9, pp. 1173–1179. © Allerton Press, Inc., 2015.
Original Russian Text © O.E. Polozhentsev, M.A. Bryleva, A.N. Kravtsova, V.K. Kochkina, A.V. Soldatov, 2015, published in Izvestiya Rossiiskoi Akademii Nauk. Seriya Fizicheskaya, 2015, Vol. 79, No. 9, pp. 1322–1328.

Icosahedral Phase Formation in an Al–Cu–Fe Quasicrystal

O. E. Polozhentsev, M. A. Bryleva, A. N. Kravtsova, V. K. Kochkina, and A. V. Soldatov

Southern Federal University, Rostov-on-Don, 344090 Russia
e-mail: olegpolozhentsev@mail.ru

Abstract—The formation of the icosahedral phase in an $Al_{70}Cu_{20}Fe_{10}$ quasicrystal and the structural transition from the crystal praphase to the quasicrystalline phase are simulated and studied by means of X-ray absorption near edge structure spectroscopy. Al–Cu–Fe samples are fabricated by means of powder metallurgy. The ω phase of the praphase crystal forms following exposure at 500°C for 20 min; the quasicrystalline phase forms after exposure at 800°C for 2 h. The model of the structural transition from the crystal to quasicrystal is a diffusion displacement of aluminum atoms around iron atoms with the formation of an icosahedron with the iron atom at the center. The immediate environment of copper atoms consists mainly of aluminum and copper atoms, and no iron atoms are observed.

DOI: 10.3103/S1062873815010256

INTRODUCTION

Quasicrystals are a new separate class of materials that, in contrast to traditional crystal structures, have no translation symmetry [1]. The icosahedral quasiperiodic structure was first encountered in rapidly quenched $Al_{86}Mn_{14}$ alloy in 1984 by D. Shechtman et al. using transmission electron spectroscopy [2]. In 2009, the authors of [3] observed natural quasicrystalline minerals for the first time. Despite having no translation symmetry, quasicrystals are characterized by long-range order, as is confirmed by sharp maxima in their diffraction patterns [4]. Quasicrystals are neither ordinary metals, insulators, nor semiconductors [5]. In contrast to insulators, they have a nonzero electron density of states at the Fermi level that is even lower than in typical metals. Among the characteristic features of a quasicrystal's electronic spectrum are a pseudogap in the electron density of states at the Fermi level and the fine peak structure reflected in the physical properties of these materials. The optical properties of quasicrystals differ from those of metals and semiconductors. Their icosahedral phase stabilizations according to the Hume–Rothery mechanism are related to the intense absorption band in the visible spectral range that is caused by excitations through the pseudogap in the excitation spectrum. The resistivity of quasicrystals is lower than that of insulators and doped semiconductors, but higher than that of metals and corresponding periodic crystal structures. Quasicrystals exhibit a variety of magnetic properties, ranging from diamagnetism to spin glass-type freezing of magnetic moments and ferromagnetic ordering. The thermal conductivity of solids and quasicrystals over a wide range of temperatures is determined by the lattice and electron contribution. The temperature dependence of the lattice conductivity of icosahedral quasicrystals differs from that of periodic crystals and amorphous materials. As was recently shown, quasicrystals exhibit the extraordinary characteristics of a fermion subsystem [6, 7]. This unique set of physical properties and the fundamentally new type of ordering in these new condensed materials have evoked great interest in them. Studies of the formation of quasicrystals as nanocluster agglomerates [8, 9] could be useful in developing new techniques for synthesizing nanostructured materials. Quasicrystal- and polymer-based composites have even greater potential [10].

Although the local atomic and electronic structures of quasicrystals can be studied using different techniques, there are no universal methods for accurately determining the parameters of the 3D distribution of atoms inside materials with no translation periodicity of their atomic arrangement. The modern level of synchrotron X-ray methods allows us to use high-resolution selective X-ray absorption spectroscopy to study small regions inside a substance. Extended X-ray absorption fine structure (EXAFS) spectroscopy has been used for some time in investigations of the radial atomic distribution in quasicrystals [11–16]. However, X-ray absorption near edge structure (XANES) spectroscopy, which yields 3D structural information on both radial and angular atomic distributions, has been used without an adequate ab initio theoretical analysis. Current advances in the theoretical analysis of experimental data allow us to develop a technique for studying the nanosized 3D geometry of quasicrystals. It was recently shown that XANES spectroscopy is quite sensitive to local variations in nanoscale structure [17]. However, since information on a fine X-ray absorption structure can be obtained only through extremely complex resource-intensive computations, researchers have so far mainly chosen one of the proposed structural models and not determined real parameters

Generalized data on the simulation of the crystal–quasicrystal structural transition using the Fitit2.0 program

Parameters	Iron's environment	Copper's environment
Coordination number	9–12	11, as in the crystal
Cluster radius for spectrum calculations	No less than 7.5 Å (124 atoms)	No less than 8.1 Å(150 atoms)
Atomic displacements in the immediate environment	Axial	No.
With atoms in the 1st coordination sphere	Only Al	Al, Cu

(atomic coordinates) for the structure of nanosized objects [18, 19].

In this work, we attempt to determine the features of the local atomic structure near iron and copper atoms in an Al_7Cu_2Fe praphase crystal and an $Al_{70}Cu_{20}Fe_{10}$ quasicrystal by means of XANES spectra analysis and computer simulation.

EXPERIMENTAL

Praphase crystal and icosahedral quasicrystal samples in the $Al_{70}Cu_{20}Fe_{10}$ system were fabricated by powder metallurgy. Aluminum, copper, and iron powders were mixed manually in isopropyl alcohol in the required proportion in an alumina mortar for an hour. The initial mixture was dried in flowing air and pressed at a pressure of 500 kg/cm^2 using the technique described in [20]. Synthesis was performed in a vacuum furnace. The ω-phase (praphase crystal) responsible for the subsequent formation of single-phase quasicrystalline $Al_{70}Cu_{20}Fe_{10}$ powder was found in our Al–Cu–Fe alloys annealed at a temperature of 550°C for 20 min. Annealing at 800°C for 2 h led to the almost complete transformation of the Al–Cu–Fe alloy into a quasicrystalline phase with an icosahedral structure, as was confirmed by X-ray analysis.

X-ray diffraction patterns were obtained on a DRON-3M diffractometer (CuK_α radiation) at Southern Federal University using the θ–2θ scanning mode in the angle range of $22° \le 2\theta \le 82°$ with a pitch of 0.02° and exposures of 8 s at each point. The X-ray tube voltage was $U = 35$ kV and the current was $I = 22$ mA. X-ray diffraction patterns were processed using the Powder Cell 2.4 software. Our investigations showed that the structure of the $Al_{70}Cu_{20}Fe_{10}$ praphase crystal corresponded to that of the analog Al_7Cu_2Fe (*P*4/*mnc* sp. gr.) crystal [21].

Fe and Cu *K*-edge XANES spectra of the investigated samples were measured on an R-XAS Looper laboratory spectrometer at Southern Federal University's Scientific and Educational Center for the Nanosized Structure of Matter. The Fe and Cu *K* edges in the $Al_{70}Cu_{20}Fe_{10}$ praphase crystal and quasicrystal were measured using a Ge(220) monochromator crystal in the transmission mode with an Ar-300 I_0 detector and an SC-70 scintillation detector. The X-ray tube voltage was $U = 25$ kV and the current was $I = 70$ mA. As a rule, the spectral quality acceptable for further quantitative analysis was obtained by averaging 4–6 independent scans for each sample. Processing the absorption spectra required determining the background function, subtracting the background from the data, determining the averaged spectra, and normalization.

The geometry of the compounds and the crystal–quasicrystal structural transition in them were simulated using the ADF program complex [22]. In simulations, the absorption spectra were calculated from the obtained atomic coordinates using the full potential finite-element method (FDMNES program complex) [23]. The structural parameters of the immediate environment were refined via multidimensional spectral interpolation using the FitIt program complex [24]. All computations were performed using the high-performance computer cluster at Southern Federal University.

RESULTS AND DISCUSSION

The Al_7Cu_2Fe crystal analogous to the $Al_{70}Cu_{20}Fe_{10}$ praphase crystal has lattice parameters $a = 6.33$ Å and $c = 14.81$ Å and the *P*4/*mnc* (no. 128) symmetry group. The $Al_{70}Cu_{20}Fe_{10}$ praphase crystal unit cell thus consists of 40 atoms (Fig. 1) in the five different positions corresponding to the three nonequivalent positions of aluminum atoms and the positions of copper and iron atoms (see table).

In the praphase crystal structure, the iron atom has the coordination number 9 and is surrounded only by aluminum atoms; the copper atom has the coordination number 11 and is surrounded by three copper atoms and eight aluminum atoms. The interatomic distances are 2.48 Å for Fe–Al, 2.53 Å for Cu–Cu, 2.56 Å for Cu–Al, and 2.86 Å for Al–Al. The Al_7Cu_2Fe praphase crystal fragment composed of several unit cells (~300 atoms) is a layered structure in which copper layers alternate with Al–Fe layers; the distance between the copper layers is ~7.5 Å and the Fe–Cu distance is ~4.19 Å.

Figure 2 presents the experimental Fe and Cu *K*-edge XANES spectra of the $Al_{70}Cu_{20}Fe_{10}$ praphase crystal and quasicrystal, along with theoretical spectra calculated by the full potential finite-element method using the FDMNES program complex. Figure 2 shows the dependence of the absorption spectra on the radius of the cluster for which the spectra were calculated.

@Элементарная ячейка кристалла Al_7Cu_2Fe

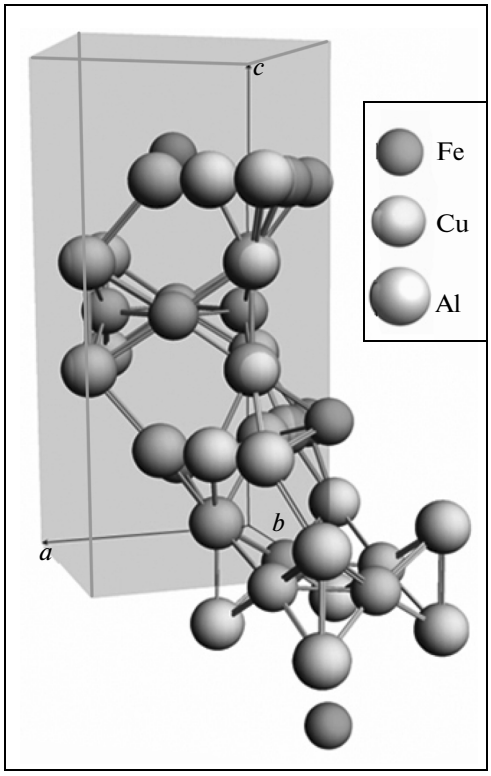

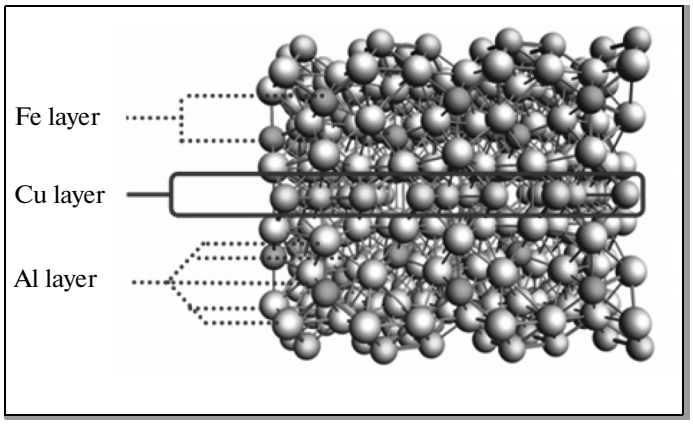

Atomic positions and coordinates in the Al_7Cu_2Fe unit cell $a = 6.33$ Å, $c = 14.81$ Å, $P4/mnc$ symmetry group [no. 128].

Atoms	Positions	*X*	*Y*	*Z*
Al(1)	4(*e*)	0.0	0.0	0.134
Al(2)	8(*g*)	0.165	0.665	0.250
Al(3)	16(*i*)	0.198	0.420	0.100
Cu	8(*h*)	0.278	0.088	0.0
Fe	4(*e*)	0.0	0.0	0.2992

Bond lengths: Fe–Al: 2.48 Å; Cu–Cu: 2.53 Å; Cu–Al: 2.56 Å; Al–Al: 2.56 Å

Fig. 1. Unit cell of the Al_7Cu_2Fe crystal, layered crystal structure, and atomic positions in the crystal unit cell.

All the features of the fine structure of the experimental Fe and Cu *K*-edge XANES spectra of the crystal are reproduced in the theoretical spectra. Since the Fe *K*-edge spectra of the crystal fragment no more than 7.5 Å in size taken from the central absorbing iron atom are similar, it is sufficient to use the radius of the cluster from the central absorbing iron atom of 7.5 Å (124 atoms for the crystal structure) in our calculations. In calculating the Cu *K*-edge spectra, it is sufficient to use a cluster radius of no more than 8.1 Å (150 atoms). These were the cluster sizes used in our calculations.

The crystal–quasicrystal structural transition was studied by means of FitIt2.0 multidimensional spectral interpolation by fitting the theoretical spectra to the experimental spectra with variations in the lengths and angles of interatomic bonds in the $Al_{70}Cu_{20}Fe_{10}$. We investigated the effect of displacements of atoms located in different coordination spheres. The shape of the EXAFS spectra changes significantly, due to the displacements of atoms located in the immediate environment of the absorbing atom in the first coordination sphere. The effect atomic displacements in the second and subsequent coordination spheres have on the shape of the spectra is negligible.

To simulate the crystal–quasicrystal structural transition, we investigated different models of atomic displacements in the first coordination spheres and chose iron and copper environmental parameters *p*1, *p*2, *p*3, *p*4, and *p*5, which can be refined through XANES analysis. The parameters were changed within physically valid limits.

We used the following crystal structure parameters in simulating the Fe *K*-edge XANES spectra of the quasicrystal (Fig. 3a): *p*1 is an increase of 10% in the distance between the Al atom and the central Fe atom; *p*2 is a 10% reduction in the distance between the Al atom and the central Fe atom; *p*3 is the different axial rotations of Al atoms around the *a*, *b*, and *c* axes; and *p*4 denotes different 10% displacements of the Fe atom from the central position in the cluster along the *a*, *b*, and *c* axes.

We used the following parameters in simulating the Cu *K*-edge XANES spectra (Fig. 3b): *p*1 is a 10% increase in the distance between the Al atom and the central Cu atom; *p*2 is a by 10% reduction in the distance between the Al atom and the central Cu atom; *p*3 denotes the different 10% displacements of neighboring Cu atoms along the *a*, *b*, and *c* axes; *p*4 is the different axial rotations of Al atoms around the *a*, *b*, and *c* axes; and *p*5 is the displacement of Al atoms relative to the copper plane.

We then investigated the dependence of the shape of the Fe*K*-edge XANES spectrum of the crystal on

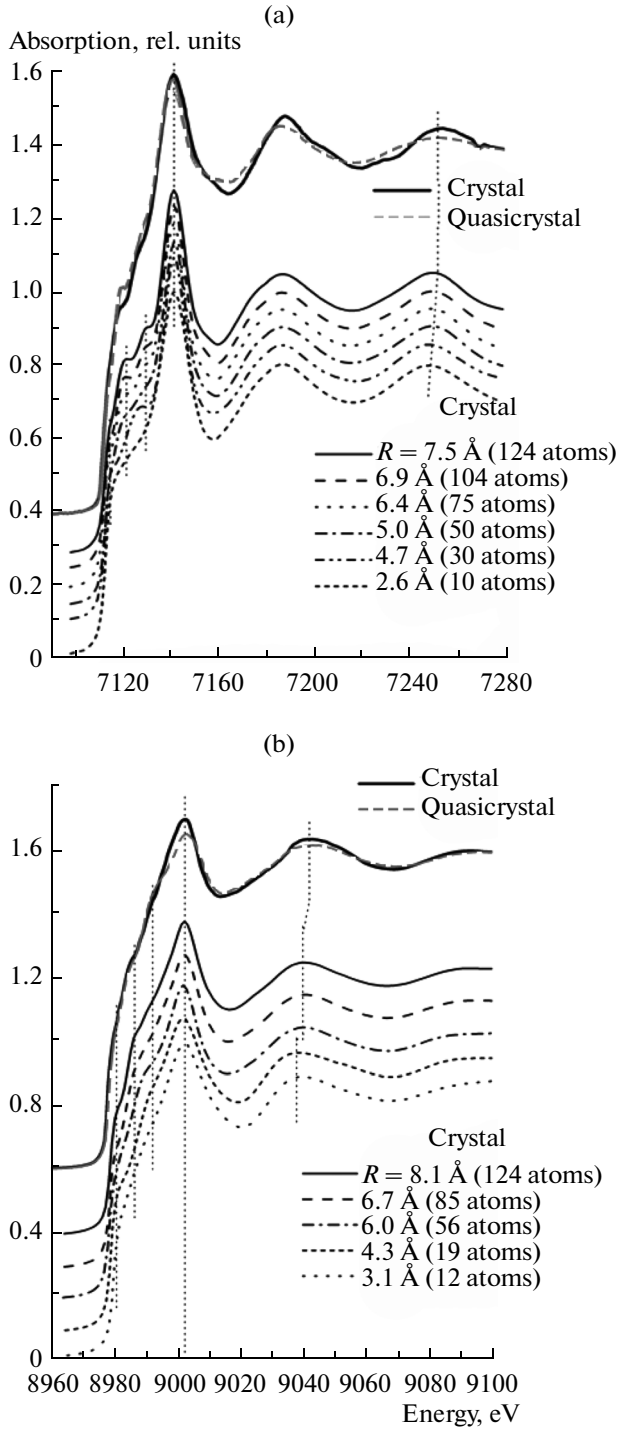

Fig. 2. Cluster radius dependence of the shape of the (a) Fe and (b) Cu *K*-edge XANES spectra of the Al–Cu–Fe crystal and quasicrystal.

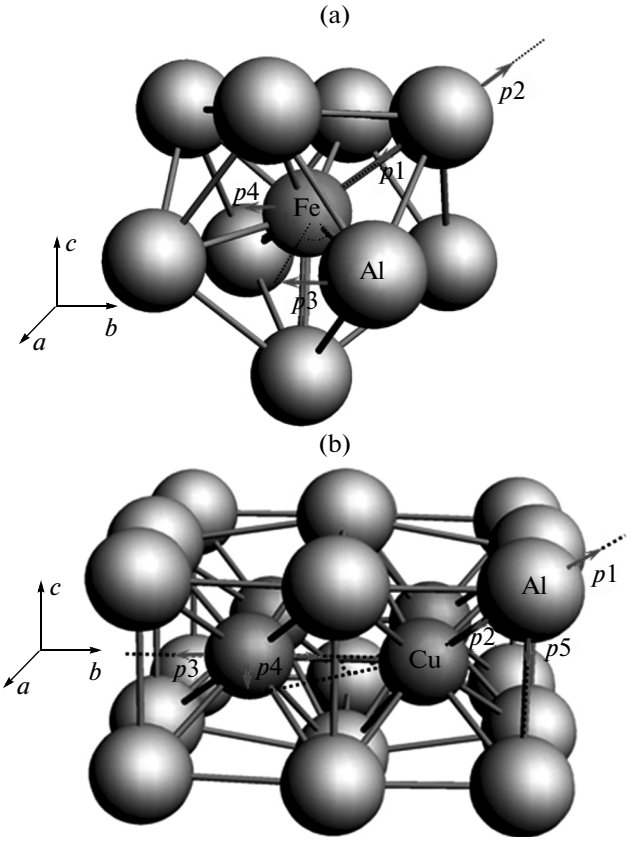

Fig. 3. First coordination sphere of (a) iron and (b) copper atoms and structural parameters that can be refined using the XANES spectroscopy data.

atomic displacements in the first coordination sphere (extension, compression, and axial displacements). We considered both single and group atomic motions (Fig. 4), the growth of the iron coordination number (Fig. 5), and the presence of copper and iron atoms in the iron's immediate environment (Fig. 6).

We investigated the variation in the shape of the Fe *K*-edge XANES spectrum of the crystal with the iron coordination number growing from 9 to 12 atoms upon the axial displacement of atoms in the immediate environment of the iron atom, where there is enough room for a larger number of atoms than in the immediate environment in the crystal (9 atoms). The number of atoms was thus raised from 9 to 12. The Al–Al, Al–Fe, and Al–Cu bonds in this case remain unstrained. We subsequently raised the number of atoms in the immediate environment and calculated the absorption spectrum of the central absorbing atom (Fig. 5). As the iron coordination number grew from 9 to 12 atoms and the atoms in the iron's immediate environment were displaced axially, the theoretical absorption spectra did not appreciably change their shape.

We studied the dependence of the shape of the Fe *K*-edge XANES spectrum of the crystal in the presence of copper and iron atoms in the iron's immediate environment (Fig. 6). The aluminum atoms in the first coordination sphere were replaced by iron and/or copper atoms and the absorption spectra were calculated with regard to these incorporated atoms. The shape of the spectrum of the central iron atom

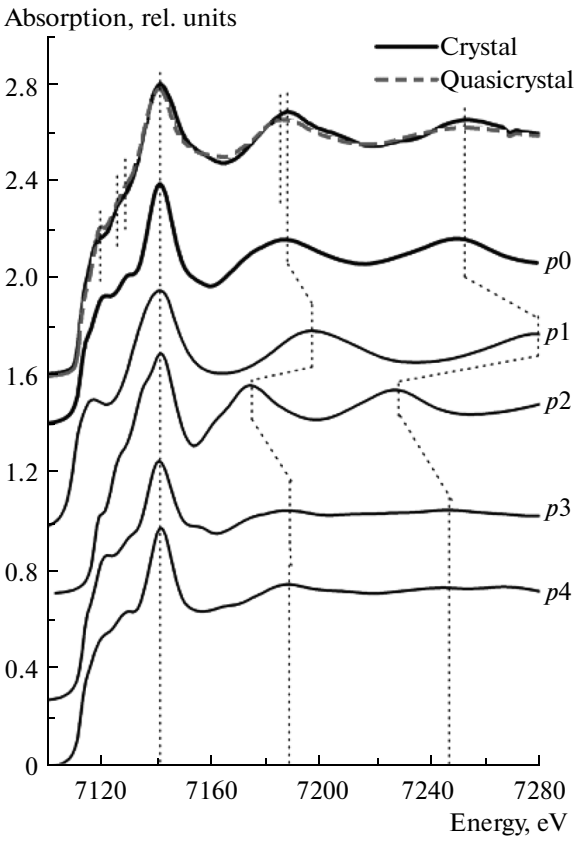

Fig. 4. Refining the parameters of the local atomic structure of an Al_7Cu_2Fe crystal via FitIt2.0 multidimensional spectral interpolation: *p*0 is the structure corresponding to the crystal; *p*1 is a 10% increase in the distance from the Al atom to the central Fe atom; *p*2 is a 10% reduction in the distance from the Al atom to the central Fe atom; *p*3 is the different axial rotations of Al atoms around the *a*, *b*, and *c* axes; *p*4 denotes different 10% displacements of the Fe atom from the central position along the *a*, *b*, and *c* axes.

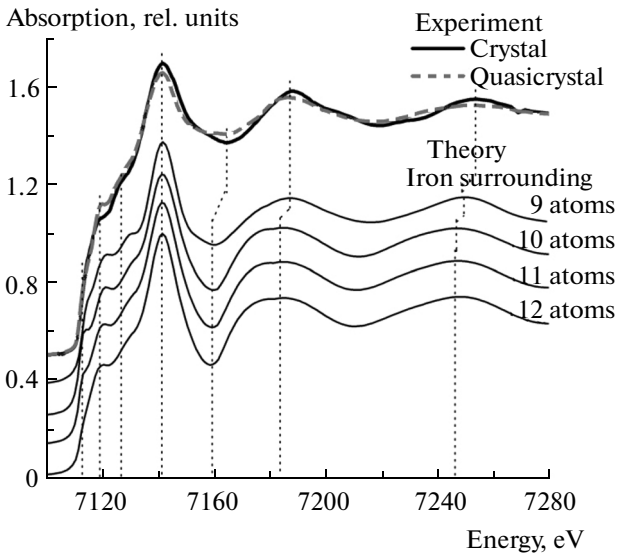

Fig. 5. Shape of the Fe *K*-edge XANES spectrum upon varying the iron coordination number from 9 to 12 atoms.

changed only slightly, while the shape of the spectrum of the incorporated iron and copper atoms changed strongly. Either the number of such atoms in the structure was very small or their environment was analogous to that of the central iron atom.

We studied the dependence of the shape of the Cu *K*-edge XANES spectrum of the crystal on atomic displacements in the first coordination sphere (extension, compression, and axial displacements of atoms; both single and group atomic motions were investigated) (Fig. 7).

The displacements of aluminum atoms (growth and reduction in the Fe–Al bond length) in the iron's immediate environment thus cannot exceed 2% of the initial length upon a crystal–quasicrystal structural transition. At the same time, large axial displacements can occur; the distance to the central atom remains invariable. The iron coordination number can grow from 9 to 12 aluminum atoms. The presence of iron and/or copper atoms in the iron's immediate environment is unlikely. Generalized data on simulations of the crystal–quasicrystal structural transition are given in the table.

Upon a crystal–quasicrystal transition, minor structural variations should occur in the immediate environment of copper atoms and the local atomic structure near copper atoms in the quasicrystal structure resembles the crystal structure; i.e., any distortion of crystal symmetry and/or atomic displacements in the immediate environment significantly change the absorption spectrum. This is not confirmed by a comparison of the experimental crystal and quasicrystal

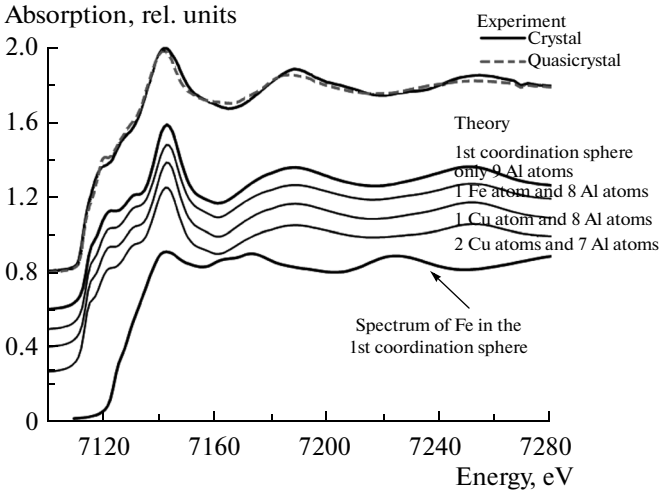

Fig. 6. Fe *K*-edge XANES spectrum of the crystal with iron and copper atoms in the first coordination sphere.

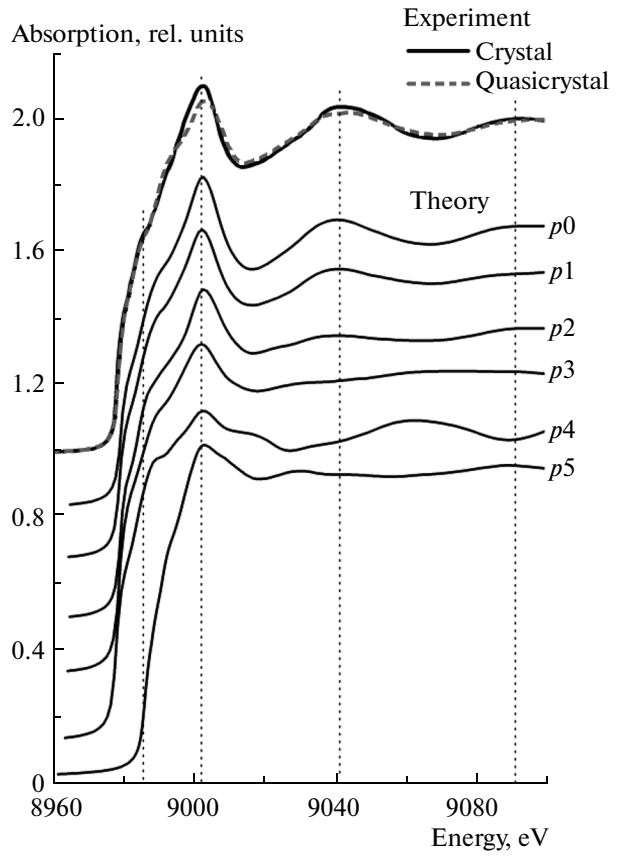

Fig. 7. Refining the parameters of the local atomic structure of an Al_7Cu_2Fe crystal via FitIt2.0 multidimensional spectral interpolation: $p0$ is the structure corresponding to the crystal; $p1$ is a 10%increase in the distance from the Al atom to the central Cu atom; $p2$ is a 10% reduction in the distance from the Al atom to the central Cu atom; $p3$ denotes the different 10% displacements of neighboring Cu atoms along the a, b, and c axes by 10%; $p4$ is the different axial rotations of Al atoms around the a, b, and c axes; and $p5$ is the displacement of Al atoms relative to the copper plane.

spectra. The presence of iron atoms in the copper immediate environment is unlikely.

Based on our analysis of the structural parameters and their effect on the spectrum shape, we propose a model for the structural transition from a crystal to a quasicrystal. In this model, the quasicrystal icosahedral symmetry forms around iron atoms, producing an icosahedron consisting of 12 aluminum atoms. The iron coordination number grows from 9 to 12 atoms. The immediate environment of copper atoms changes insignificantly and the formation of the icosahedral surrounding in the iron local surrounding alters the copper's immediate environment. Copper atoms are not displaced from the plane and aluminum atoms neither distort nor penetrate it.

CONCLUSIONS

The formation of the quasicrystal icosahedral structure from the $Al_{70}Cu_{20}Fe_{10}$ praphase crystal fabricated by powder metallurgy was simulated. Using XANES spectroscopy data, the possibility of forming the icosahedral environment of an iron atom using only aluminum atoms was studied. In this case, copper atoms retain their symmetry analogous to that of a praphase crystal. The dependence of the shape of the Fe and Cu K-edge XANES spectra of the crystal on atomic displacements (extension, compression, and axial displacements) in the first coordination sphere was investigated. Both single and group atomic motions, the growth of the iron coordination number, and the presence of copper and iron atoms in the iron's immediate environment were considered. Our model of the structural transition from a crystal to a quasicrystal is thus a diffusion displacement of aluminum atoms around an iron atom, followed by the formation of an icosahedron with the iron atom at the center. The immediate environment of copper atoms consists mainly of aluminum and copper atoms; iron atoms are not found in the copper's immediate environment.

ACKNOWLEDGMENTS

We would like to thank the team led by A.A. Teplov at the Kurchatov Institute in Moscow for providing our Al–Cu–Fe praphase crystal and quasicrystal samples. Our calculations were performed at the South Russia Regional Informatization Center of Southern Federal University.

This work was supported by the Russian Foundation for Basic Research, project no. 14-02-31514-mol_a.

REFERENCES

1. Vekilov, Yu.Kh. and Chernikov, M.A., *Phys.-Usp.*, 2010, vol. 53, no. 6, p. 537.
2. Shechtman, D., Blech, I.A., Gratias, D., and Cahn, J.W., *Phys. Rev. Lett.*, 1984, vol. 53, p. 1951.
3. Bindi, I., Steinhardt, P.J., Yao, N., and Lu, P.J., *Science*, 2009, vol. 324, p. 1306.
4. Steinhardt, P.J., *Rend. Lincei*, 2013, vol. 24, p. S85.
5. Tsai, A.-P., *Chem. Soc. Rev.*, 2013, vol. 42, p. 5352.
6. Shaginyan, V.R., Msezane, A.Z., Popov, K.G., Japaridze, G.S., and Khodel, V.A., *Phys. Rev. B*, 2013, vol. 87, p. 245122.
7. Timusk, T. and Carbotte, J.P., *Phys. Rev. B*, 2013, vol. 87, p. 235121.
8. Abe, E., Yan, Ya., and Pennycook, S.J., *Nat. Mater.*, 2004, vol. 3, p. 759.
9. Van Blaaderen, A., *Nature*, 2009, vol. 451, p. 892.
10. Kenzari, S., Bonina, D., Dubois, J.M., and Fournee, V., *Mater. Des.*, 2012, vol. 35, p. 691.
11. Sadoc, A., *J. Phys.,* 1986, vol. 47, p. C8-1003.

12. Saksl, K., Vojtech, D. and Franz, G., *J. Mater. Sci.*, 2007, vol. 42, p. 7198.
13. Sadoc, A., Flank, A.M., and Lagarde, P., *Philos. Mag. B*, 1988, vol. 57, no. 3, p. 399.
14. Sadoc, A., Itie, J.P., Polian, A., and Lefebvre, S., *J. Phys. (Paris)*, 1997, vol. 7, p. C2-991.
15. Takakura, H., Gomez, C.P., Yamamoto, A., De Boissiu, M., and Tsai, A.P., *Nat. Mater.*, 2007, vol. 6, p. 58.
16. Menushenkov, A.P. and Rakshun, Ya.V., *Crystallogr. Rep.*, 2007, vol. 52, no. 6, p. 1006.
17. Soldatov, A.V., *J. Struct. Chem.*, 2008, vol. 49, p. 111.
18. Léon, A., Yalovega, G., Soldatov, A., and Fichtner, M., *J. Phys. Chem.*, 2008, vol. 112, p. 12545.
19. Evsyukova, M.A., Yalovega, G., Balerna, A., Menushenkov, A.P., Rakshun, Ya.V., Teplov, A.A., Mikheeva, M.N., and Soldatov, A.V., *Phys. B*, 2010, vol. 405, no. 8, p. 2122.
20. Bryazkalo, A.M., Laskova, G.V., Mikheeva, M.N., Sumarokov, V.N., and Teplov, A.A., in *Sbornik dokladov I vserossiiskogo soveshchaniya po kvazikristallam* (Proc. 1st All-Russian Meeting on Quasicrystals), Moscow, 2003, p. 35.
21. Trambly, G., Dankhazi, Z., Belin, E., Sadoc, A., Manh Duc, N., Mayou, D., Keegan, M.A., and Papaconstantopoulos, D.A., *Phys. Rev. B*, 1995, vol. 51, no. 20, p. 14035.
22. ADF2009.01, http://www.scm.com
23. Joly, Y., *Phys. Rev. B*, 2001, vol. 63, p. 125120.
24. Smolentsev, G. and Soldatov, A.V., *Comput. Mater. Sci.*, 2007, vol. 39, p. 569.

Translated by E.V. Bondareva